Fully-coupled numerical model for ballasted track analysis – Field measurements and predictions

R. Mezeh, Hussein Mroueh, M. Hosseingholian, Marwan Sadek

▶ **To cite this version:**

R. Mezeh, Hussein Mroueh, M. Hosseingholian, Marwan Sadek. Fully-coupled numerical model for ballasted track analysis – Field measurements and predictions. Transportation Geotechnics, 2021, 27, 10.1016/j.trgeo.2020.100483 . hal-03256549

HAL Id: hal-03256549
https://hal.science/hal-03256549v1

Submitted on 2 Jan 2023

HAL is a multi-disciplinary open access archive for the deposit and dissemination of scientific research documents, whether they are published or not. The documents may come from teaching and research institutions in France or abroad, or from public or private research centers.

L'archive ouverte pluridisciplinaire **HAL**, est destinée au dépôt et à la diffusion de documents scientifiques de niveau recherche, publiés ou non, émanant des établissements d'enseignement et de recherche français ou étrangers, des laboratoires publics ou privés.

Distributed under a Creative Commons Attribution - NonCommercial 4.0 International License

Version of Record: https://www.sciencedirect.com/science/article/pii/S2214391220303718
Manuscript_1f2fd63510f0bcba77bd64b27f23b6ec

Fully-coupled numerical model for ballasted track analysis – Field measurements and predictions

Reda Mezeh [1,2], Hussein Mroueh* [1], Mohsen Hosseingholian[2], Marwan Sadek[1]

(1) University of Lille, IMT Lille Douai, Univ. Artois, Yncrea Hauts-de-France, ULR 4515 - LGCgE, Laboratoire de Génie Civil et géo-Environnement, F-59000 Lille, France.

(2) IRT Railenium, F-59300 Famars, France

* Corresponding Author

Abstract

This paper proposes a three-dimensional fully-coupled numerical model intended for the simulation of the dynamic behavior of ballasted railway tracks under real excitation. It is employed to reproduce the response of a French site located at the high-speed line connecting the two regions Bretagne and Pays de la Loire. The equation of motion is solved in the time domain by means of the finite difference method in which the rails and sleepers are represented by rectilinear beam elements which are rigidly attached to a spatial grid composed of rectangular cuboids. An adaptive meshing scheme based on the creation of load-attached moving nodes is adopted to model the moving train loads which are supposed to be time-independent. To validate the numerical simulations, a measuring campaign is performed in which tow aligned deflectometers are used to measure the displacement of the railway foundation just below the ballast layer under the track centerline. The velocity range of the high-speed passenger trains is covered in which four cases are taken into consideration ranging from 162 to 342 km/h. An excellent agreement between measurements and predictions is found. Therefore, the presented model can be considered reliable for the design of new high-speed lines.

Keywords: field measurements; 3D modeling; track response; adaptive mesh; ballasted track

© 2020 published by Elsevier. This manuscript is made available under the CC BY NC user license
https://creativecommons.org/licenses/by-nc/4.0/

1. Introduction

In dense cities the noise and vibrations induced by high-speed trains (HST) are considered as a major source of inhabitants' disturbance. The continuous expansion of urban agglomerations has forced the city planners to bring the residential buildings closer to the high-speed lines (HSL). Typically, in the frequency range 1-80 Hz, the ground-borne vibration is considered as feelable whole-body vibration that can disrupt the functioning of sensitive equipment [1]. Therefore, the study of the excitation mechanisms of the railway track systems as well as the propagation pattern of the induced vibrations is of high importance. In addition to the environmental impact, we should not ignore the economic side of this study that can lead to significantly decrease the project cost by proposing alternative track formations.

With the fast development of computing tools, the numerical solving in the time domain of the train/track/ground coupled problem has become possible. Many researches and literature surveys on the behavior of the high-speed rail systems have been published [2–4]. The impact of the embankment dimensions and stiffness of track components on the vertical deflection of ballasted railway tracks was addressed by Real et al. [5]. In their study, a sensitivity analysis was conducted to assess the influence of the different geo-mechanical track parameters. Then, by taking into consideration the significant variables, a multiple regression analysis was carried out using the three-dimensional (3D) finite-element (FE) simulations. For design purposes, the vertical stiffness of the track has a major impact on the dynamic behavior of the system under moving loads. In general, to reduce the track deterioration, high bearing resistance is needed. On the other hand, relatively high track stiffness leads to increase the dynamic loads on the rail and subsequently the induced acceleration that can prejudice the passengers comfort. In this context, Gallego Giner and Lopez Pita [6] studied the dynamic behavior of embankment-structure transitions using FE modeling in order to improve the methods available for the design of railway tracks. Thompson et al. [7] approached the problem of interrupting the transmission path of ground-borne vibration from surface railways. They used a 2.5D coupled finite-element/boundary-element methodology to investigate the effects of subgrade stiffening, either directly under the track or at some depth, on the vibration level at sites with soft grounds. This technique was found to significantly mitigate the vibrations above around 20 Hz for the soil configuration with 3 m deep soft layer and above around 10 Hz for a 6 m layer. Grabe [8] and Grabe and Clayton [9] indicated that the dynamic effects could be ignored, in which static analysis might be considered sufficient, for speeds up to 240 km/h on a firm subgrade. In this context, Yang et al. [10] investigated the effective resilient stiffness of subgrade which depends on the stress state of the ground and the stress path followed during loading by means of a two-dimensional dynamic FE analysis. They studied the effects of train speed, acceleration/braking, geometric variation in rail head level and a single unsupported sleeper on the dynamic response of the subgrade. They found that when the train speed reaches the half of the Rayleigh wave speed, the shear stresses will be underestimated by 30% in a static analysis, and the dynamic effects increase dramatically with the increasing of train speed. As mentioned by Madshus and Kaynia [11], the Rayleigh wave velocity of peats and soft clays could reach 40-50 m/s.

Alves Costa et al. [12] presented a 2.5D numerical model based on equivalent linear analysis and coupled with iterative procedure to take into account the soil non-linearity. They have

validated their model by simulating the HSL of Ledsgård in Sweden, from which extensive measurements are available from the late 1990s, and considering several circulation speeds for the X2000 train. Shih et al. [13] have studied the deflection of the HSL of Ledsgårde under the loads of moving trains using a FE model in which a reduction law of the shear modulus of soil according to the octahedral shear strain was considered. In addition, they proposed an equivalent linear model in which they recommended the use of an equivalent soil modulus that corresponds to 20% of the maximum strain (effective strain) rather than the value of 65% commonly used in earthquake studies. In this context, Hegde and Sitharam [14] have performed experimental and 3D numerical studies using FLAC3D to enhance the mechanical behavior of soft clay bed. They have investigated three types of reinforcements: geogrid cells, commercial geocells and the bamboo cells, in which due to its higher stiffness, higher tensile strength and the higher surface roughness values, the maximum bearing capacity was observed in the case of foundation bed reinforced with the bamboo cells.
Later, Mezeh et al. [15] proposed an experimentally validated 1D model consisting of infinite Euler-Bernoulli beam that rests on continuous viscoelastic foundation. The model parameters including foundation impedance and wheel/rail interaction length were calibrated using an iterative curve fitting procedure in the velocity range 162–342 km/h. The experimental data was collected from an instrumented segment on the "Bretagne" - "Pays de la Loire" (BPL) HSL. Regarding to the involved degrees of freedom and the required computational effort, the efficiency of the proposed model could be considered high.

The structural and acoustic response to high-speed surface railway traffic excitation, of a multi-story portal frame was studied by Fiala et al. [16]. They divided the problem into three weakly coupled sub-problems in which the first aims to find the free-field ground displacements induced by the passage of a HST. The incident wave field is then used to excite a coupled soil-structure model (second sub-problem) in order to find the response of the structure. Finally, the obtained structural vibrations are used to compute the ground-borne noise in the structure's enclosures. Sayeed et al. [17] investigated the critical speed of moving trains at which the dynamic response of the ballasted railway track reaches a peak and related it to the theoretical Rayleigh-wave velocities of the geo-materials. Recently, Li et al. [18] developed a 3D model incorporating FE meshes coupled with infinite element boundaries for the simulation of the dynamic response of ballasted railway under moving HST excitation. They validated the 3D numerical tool by comparison against the results of Euler-Bernoulli beam model. However, in order to ensure credibility to the numerical predictions, field measurements are required.

This paper presents a fully-coupled 3D numerical model for the simulation of the behavior of ballasted railways under dynamic loading. A spatiotemporal finite-difference formulation which has been developed by Mezeh et al. [19] is employed to represent the load diffusion through the track structure to the sub-soil layer. To model the applied moving loads, an adaptive meshing scheme is used in which it is based upon the creation of load-attached moving nodes, hence the name: L-AMN approach. The excellent performance of the adopted step-by-step procedure when modeling the mutual dynamic interactions between the various components of the track system has been highlighted in the reference [19]. Real-scale experimental measurements on track vibration from a French site with various traveling speeds of a passenger HST are employed to validate the model. The considered site which is located on the Bretagne-

Pays de la Loire (BPL) HSL, in the west of France, consists of longitudinally invariant rectilinear track with classical ballasted formation composed of: ballast, sub-ballast (untreated gravels) and sub-base (treated gravels) layers. Vertical displacement histories recorded by two anchored deflectometers placed just below the ballast layer under the track longitudinal centerline are used to verify the credibility of the geo-mechanical properties of the model. The field measurements are compared with those predicted by the 3D interaction model for various velocities of the passenger HST that ranging from 162 to 342 km/h. The proposed model is then used to investigate the dynamic responses of the rails as well as the top of the ballast and sub-base layers (between the rails). It shows an important capacity for the computation of the free-field ground displacements induced by the passage of a moving HST.

The structure of the text is as follows: Section 2 presents the instrumented site with the dimensions and axle loads of the HST which is assumed to cross the track at constant speed. Also, it explains the preliminary treatment of the measurements that leads to find the velocity of each HST passage. Section 3 describes the 3D numerical model including the applied recommendations for accurate modeling of the induced waves which take place at the wheel/rail interface and reach the ground through the track formation. Section 4 presents the confrontation between the numerical predictions and the experimental measurements in terms of vertical displacement field of the base of the ballast layer. Finally, section 5 discusses and critically evaluates the obtained results.

2. Instrumented track (BPL project)

In order to improve the accessibility of the line "Grand ouest" within the French high-speed rail network, an extension of the existing HSL between Paris and Connerré (20 km east of Le Mans) was proposed in which the construction was started in July 2012. Indicatively, Figure 1 illustrates one of the first phases of project execution: earthworks. The implemented HSL puts Rennes less than 1h30 from Paris by crossing the two French regions Bretagne and Pays de la Loire over a total length of 182 km; hence the name BPL. Figure 2 shows the rail network in the study area.

Location of Figure 1

Location of Figure 2

Within the frame of this cooperative project, the dynamic behavior of an instrumented section of the HSL is investigated under real excitation for several cases of train traveling velocity V. Figure 3 presents the transversal section of the studied ballasted track. It consists of a ballast bed that rests on an untreated gravels layer, supporting two parallel rectilinear rails by means of uniformly spaced horizontal sleepers. The center-to-center distance between the mono-block concrete sleepers is fixed at 0.6 m. The transition to the homogeneous sub-soil half-space is ensured by a cement-treated sub-base layer.

Location of Figure 3

In this work, the railway traffic that occurred during the period between November and December 2016 (test period) is considered in which a unique passenger HST, with a total mass

of 380 tons, was employed. It is composed of 2 traction cars, 2 end carriages and 6 central carriages included a wagon bar. The modular subassembly of the axles is ensured by 13 bogies in which their wheelbase is $E = 3\ m$. The dimensions of the train and the position of each axle are presented in Figure 4. Noting that, the transmitted loads by the train to the track are determined by means of static weighing of vehicles; the obtained values are summarized in Table 1.

Location of Figure 4 [20]

Table 1 Transmitted load per each axle for the employed high-speed train (French TGV)

Axle position	Axle load (tons)
Bogies of the traction cars	17.0
Extreme bogies (2 end carriages)	12.0
Intermediate bogies	14.5
Bar wagon bogies	15.5

2.1. Measuring campaign

Since January 2015, the instrumentation of a rectilinear section made of classical ballasted formation is done as the construction work progresses. As shown in Figure 5, accelerometers, temperature probes, strain gauges, anchored deflectometers and humidity probes are employed to understand what happens when the track is loaded. The sensors are connected to an energy-autonomous acquisition system which supplies the site by power and allows the interrogation and scaling of the measuring tools. Acquired data are transmitted in real time via remote server and the access to the measures is ensured by means of a web application.

Location of Figure 5

The present study focuses only on the measurements provided by the two aligned deflectometers that are employed to assess the railway foundation displacement at the top of the untreated gravels layer. In the field, each deflectometer is attached to an anchored rod in such a way that the rod base is located below the zone of influence of the applied loads. Therefore, the relative displacement between the rod and the senor is none other than the displacement of the point where the sensor is located.

2.2. Data treatment

Before using the field measurements, a preliminary treatment is performed to remove the noise using a low-pass filter with a velocity-dependent cutoff frequency taken as the double of the axle passing frequency f_{ap} which is expressed as follows:

$$f_{ap} = \frac{V}{E} \tag{1}$$

Figure 6 shows the impact of the filtering process on a measured signal of rail-foundation displacement designated in the following by *y*.

Location of Figure 6

Seen that, the distance along the track centerline between the two aligned deflectometers, 1 and 2, is known ($d = 7m$), the velocity of the moving HST can be determined from the time delay between the two measured signals [21]. Therefore, by looking for downward zero-crossings in the first derivative that exceed a predefined threshold, the peaks (moment of arriving of wheels) of the filtered signals are detected. Then, from the time lag Δt_j between the jth peak of each signal, V is determined by taking the average of the values obtained from the 26 wheels; it is expressed as follows:

$$V = \frac{d}{26}\sum_{j=1}^{26}\frac{1}{\Delta t_j} \tag{2}$$

In the sequel, for each HST passage, the mean of the two displacement signals (after synchronization) is considered.

In order to cover the velocity range of the high-speed passenger trains, four cases are taken into account that of $\mathrm{V} = 162, 200, 300$ and $342\ \mathrm{km/h}$. Note that, Figure 6 corresponds to $\mathrm{V} = 342\ \mathrm{km/h}$.

3. Numerical modeling of the site

This work aims to provide a reliable modeling of the railway track dynamics by considering the mutual interactions between the different components of the system. The loads transmission from the wheel/rail interface to the track formation, with all its mechanical heterogeneity, and from there to the nearby structures through the subgrade, involves a complex dynamic problem. Moreover, in order to reproduce the real situation, several factors should be considered especially the long-term behavior of the constitutive materials, i.e. residual displacements, ballast deterioration, fatigue strength…, as well as the wheel/rail roughness and track unevenness. In addition to that, some numerical complications appear when modeling the moving loads problem using either the finite element or finite difference method mainly when the traveling velocity is high or/and the loads contain high-frequency components.

In this work, we admit that the constitutive materials of the track as well as the subgrade layer behave elastically with small strain levels. Table 2 gives the elastic properties of the granular materials; where E, v and ρ are the Young's modulus, Poisson's ratio and material density respectively. Furthermore, the mechanical parameters of the continuous welded rail which lay at 1.435 m gauge, are given in Table 3; where I_Y and I_Z are the second moment of inertia around Y-axis (transversal direction) and Z-axis (vertical direction) respectively and J_X is the torsional stiffness around X-axis (longitudinal direction).

Table 2 Elastic parameters of the granular materials

Layer	$E\ (MPa)$	ν	$\rho\ (kg/m^3)$
Ballast	120	0.40	1600
Untreated gravels	160	0.35	1600
Cement-treated gravels	700	0.35	2000

Sub-soil	150	0.35	1800

Table 3 Elastic parameters of the continuous welded rail

$E\ (GPa)$	ν	$I_Y(m^4)$	$I_Z(m^4)$	$J_X(m^4)$	$Area\ (m^2)$	$\rho(kg.m^{-3})$
200	0.30	3.055e-5	5.13e-6	1.6975e-5	7.686e-3	7850

3.1. Computational grid

The finite difference explicit code FLAC^{3D} is employed to perform the numerical modeling in the time domain. Eight-noded brick elements are used to discretize the substructure of the railway consisting of: ballast, untreated gravels, sub-base and sub-soil layers. On the other hand, the rails and sleepers are modeled using rectilinear beam elements in which each finite element is composed of two nodes with six degrees of freedom per node and is rigidly connected to the grid such that both entities behave elastically with non-failure limit. Figure 7 illustrates an example of the three-dimensional spatial mesh which can be used to assess the response of each component of the system. It should be mentioned that the symmetry condition is enforced along the vertical plane $(\overrightarrow{OX}, \overrightarrow{OZ})$ by virtue of the fact that the loads are assumed to be applied equally on each rail. Consequently, the half of the transversal section is considered which leads to reduce the required resolution time and the necessary memory allocation. On the other hand, regarding the model dimensions, enough length and width are adopted to reduce the negative effect of spurious reflections at the model boundaries on the numerical calculation. Moreover, in order to damp the residual non-dissipated waves, absorbing boundary condition insured by viscous dampers [22] is imposed at the three other vertical sides. Noting that, the sub-soil layer is assumed to overlay bedrock. Thus, fixed boundary condition is applied at the base of the model.

Location of Figure 7

To accurately simulate the response of the track/ground system under HST excitation, a graded mesh is considered in which the size Δl of the finite elements that are close to the loads path is determined according to the recommendations provided by the study of Mezeh et al. [19]. Consequently, the critical wavelength associated with the highest frequency component f_{sup} is represented by 14 brick elements. Thus, Δl is given by the following equation:

$$\Delta l = \frac{C_s}{14.f_{sup}} \tag{3}$$

where C_s is the shear wave (S-wave) speed in the most flexible foundation layer and f_{sup} is taken as the axle passing frequency f_{ap}.

3.2. Loading of the system

The numerical techniques employed to model the moving loads problem and obtained from a reformulation of the finite element or finite difference methods can be classified into two

categories. The first one is based upon a time-domain formulation in a fixed spatial reference system [23,24] while the second one is composed from methods formulated in a load-attached moving reference system (Moving Element Method MEM [25], Periodic Configuration Update PCU method [26] …). However, the performance of the first approach is highly impacted by the mesh of the computational grid and in most cases of dynamic loading it requires a refined domain to achieve acceptable accuracy. Unfortunately, this fact leads to large increase in the calculation time. On the other hand, when the geometry or/and the behavior of the system are complex, the second approach becomes complicated and requires the consideration of simplifying assumptions before being used.

In this work, the numerical scheme "L-AMN" proposed by Mezeh et al. [19] is adopted to model the moving HST loads. It is based upon the creation of load-attached moving nodes on the rail rolling surface to produce local spatial refinement. Subsequently, it ensures a much better representation of the moving loads effect with respect to other classical methods. The equation of structural dynamics providing the bending deformation is solved in the time domain via step-by-step mesh adaptation mechanism of the rail in which the system is assumed to be subjected to a stationary loading during each calculation step. As shown in Figure 8, within the frame of this approach, each two-noded beam element of length l located on the loads trajectory is divided into S_x subdivisions in which Δt represents the required time to cross each subdivision at constant velocity V:

$$\Delta t = \frac{l}{S_x . V} \tag{4}$$

At time t, the moving load is considered to be applied at the left node (the load motion is from left to right) of the finite element i. It remains at the same position until time $t + \Delta t$ in which a first temporary node is injected into the grid, so that the load moves towards it. It remains loaded as long it exists, before being deleted allowing to create a neighbor temporary node, and so on. This adaptive meshing process which is formulated in a fixed reference system gives rise to the concept of "moving node". It should be mentioned that, at the end of each calculation step, namely at time $t + j.\Delta t$ such as $1 \leq j \leq S_x - 1$, the position of the jth temporary node is initialized using the Hermite's interpolating polynomial which ensures both the deflection and slope compatibility on the adjacent elements. Therefore, the cubic polynomials representing the vertical displacement u and the plane rotation θ fields in the local reference system x_l of the loaded finite element are:

$$u(x_l) = N_1 u_h + N_2 \theta_h + N_3 u_{i+1} + N_4 \theta_{i+1} \tag{5a}$$

$$\theta(x_l) = N'_1 u_h + N'_2 \theta_h + N'_3 u_{i+1} + N'_4 \theta_{i+1} \tag{5b}$$

Noting that the index h which appears in the previous equations denotes the left node of the temporary finite element; it is given as follows:

$$h = \begin{cases} i & if \quad j = 1 \\ j - 1 & otherwise \end{cases} \tag{6}$$

Location of Figure 8

Subsequently, at time $t + j.\Delta t$, the total length l_e of the temporary finite element which is delimited between the nodes h and $i + 1$ is given as follows:

$$l_e = l - (j - 1)\frac{l}{S_x} \tag{7}$$

On the other hand N_k $(1 \leq k \leq 4)$ are the shape functions; they are expressed according to the dimensionless variable r as follows:

$$N_1 = 1 - 3r^2 + 2r^3 \tag{8a}$$

$$N_2 = (r - 2r^2 + r^3)l_e \tag{8b}$$

$$N_3 = 3r^2 - 2r^3 \tag{8c}$$

$$N_4 = (-r^2 + r^3)l_e \tag{8d}$$

where r denotes the relative distance along the temporary finite element:

$$r = \frac{x_l}{l_e} \tag{9}$$

Finally, after replacing x_l by $V.\Delta t$, the vertical displacement u_j and the plane rotation θ_j at the upcoming temporary node j can be determined using Eqs. 5a and 5b respectively. Note that, similar equations are employed to initialize the linear and angular velocities (denoted respectively by $\dot{u}_j$ and $\dot{\theta}_j$) based on the reached equilibrium state of the system at the end of the calculation step $[t + (j - 1).\Delta t, t + j.\Delta t]$:

$$\dot{u}_j = N_1\dot{u}_h + N_2\dot{\theta}_h + N_3\dot{u}_{i+1} + N_4\dot{\theta}_{i+1} \qquad /x_l = V.\Delta t \tag{10a}$$

$$\dot{\theta}_j = N'_1\dot{u}_h + N'_2\dot{\theta}_h + N'_3\dot{u}_{i+1} + N'_4\dot{\theta}_{i+1} \quad /x_l = V.\Delta t \tag{10b}$$

It should be mentioned that, this process can be generalized to model the passage of multiple moving loads via the creation of multiple moving nodes. For further details about the L-AMN

approach, we refer the reader to the reference [19] which presents a complete study covering the formulation and the validation of the approach.

4. Predictions versus measured signals

This section aims to investigate the capacity of the proposed model to represent the mutual dynamic interactions between the various components of the high-speed rail system, by means of linking the collected measurements to the numerical predictions. As a result of lengthy calibration process, the mechanical parameters needed to launch the 3D simulations are determined; they are presented in Table 2. Due to the spatiotemporal adaptive mesh of the rails which ensures a reliable modeling of the moving loads, both the quasi-static and the inertial components of the dynamic response of the system are taken into consideration. The system is excited by the passage of two consecutive bogies: the first supports the traction car while the second is an extreme bogie, crossing the perfectly-smooth rails at constant velocity. Figures 9 to 12 show the confrontation between the predicted and the measured responses of the ballasted foundation under the track centerline in which they correspond to $\mathrm{V} = 162, 200, 300$ and $342\ \mathrm{km/h}$ respectively. In order to better understand the mechanism of interaction between the HST, the track formation and the homogeneous supporting sub-soil, the fast Fourier transform (FFT) is employed to switch from the time-axis to the frequency-axis. Therefore, for each case of study, the frequency content of the displacement signal is presented.

Location of Figure 9

Location of Figure 10

Location of Figure 11

Location of Figure 12

The obtained results prove the potentiality of the 3D model to reproduce the dynamic response of the French site in which for the various cases of V the predicted and the measured signals show an excellent similitude (phase and amplitude) in the time and frequency axis. On the other hand, the frequency contents of the various displacement signals show that the quasi static contribution dominants the dynamic contribution in which the axle passing frequency (Eq. 1) appears with small amplitude compared to that corresponding to $f = 0$. However, several parameters could amplify the dynamic contribution like wheel/rail irregularity, track unevenness and the presence of transition zone on the HST path.

Much information about the system components could be derived from the numerical calculations as the rail deflection u, the response of each layer of track formation and the spatial spread of the induced waves. Moreover, the impact of the geo-mechanical parameters of the site could be studied. In this context, Figure 13 presents the rail deflection history that corresponds to $V = 162\ km/h$. It can be used to find the equivalent vertical stiffness of the railway $\bar{k}$ which is defined as the ratio between the applied vertical load Q and u:

$$\bar{k} = \frac{Q}{u} \tag{11}$$

Location of Figure 13

It can be concluded that for the studied French site, the average value of the vertical stiffness is around $180\ kN/mm$.

Concerning the spatial spread of the ground-borne vibration along the homogeneous half-space, Figure 14 illustrates the obtained contours of the Z-displacement for the case of $V = 162\ km/h$.

Location of Figure 14

According to the obtained results, the fully-coupled finite difference model which is coupled in the time domain with an adaptive meshing scheme (L-AMN approach) can be considered reliable to analyze the behavior of ballasted tracks.

5. Conclusion

The work presented in this paper explores the performance of a finite difference model dedicated to simulate the dynamic response of high-speed train/track/ground system. The computational model consists of a three-dimensional grid coupled with an adaptive meshing scheme (L-AMN approach) which has been used to model the loading process of the system via the creation of load-attached moving nodes. Both, inertial and quasi-static effects of the moving loads crossing the rails at constant velocity have been taken into consideration in the linear elastic domain. Displacement histories of the railway foundation that were recorded at the high-speed line connecting the two French regions: Bretagne and Pays de la Loire (west of France), have been used to validate the numerical model. Several traveling velocities of a passenger HST with deterministic transferred loads to the track have been considered ranging from 162 to 342 km/h. An excellent agreement has been found between the predicted and the measured responses of the ballasted foundation under real excitation. This study has been proved the potentiality of the numerical model which can be used to check the rules applied for railways design. Thus, alternative recommendations could be proposed for researchers and practitioners working in railways field.

Acknowledgments

The present research was supported by the IRT Railenium and University of Lille (LGCgE) within the project: 'High-speed line Bretagne-Pays de la Loire BPL'. The first author wants to acknowledge the valuable discussions had with the partners: SNCF Réseau - The French national railway network company, EIFFAGE Infrastructures company, IFSTTAR and SETEC Ferroviaire company.

References

[1] Jones CJC, Block JR. PREDICTION OF GROUND VIBRATION FROM FREIGHT TRAINS. J Sound Vib 1996;193:205–13. https://doi.org/10.1006/jsvi.1996.0260.

[2] Wu J-S, Shih P-Y. DYNAMIC RESPONSES OF RAILWAY AND CARRIAGE UNDER THE HIGH-SPEED MOVING LOADS. J Sound Vib 2000;236:61–87. https://doi.org/10.1006/jsvi.2000.2959.

[3] Wu TX, Thompson DJ. VIBRATION ANALYSIS OF RAILWAY TRACK WITH MULTIPLE WHEELS ON THE RAIL. J Sound Vib 2001;239:69–97. https://doi.org/10.1006/jsvi.2000.3157.

[4] Connolly DP, Kouroussis G, Laghrouche O, Ho CL, Forde MC. Benchmarking railway vibrations – Track, vehicle, ground and building effects. Constr Build Mater 2015;92:64–81. https://doi.org/10.1016/j.conbuildmat.2014.07.042.

[5] Real JI, Gómez L, Montalbán L, Real T. Study of the influence of geometrical and mechanical parameters on ballasted railway tracks design. J Mech Sci Technol 2012;26:2837–44. https://doi.org/10.1007/s12206-012-0734-7.

[6] Gallego Giner I, López Pita A. Numerical simulation of embankment—structure transition design. Proc Inst Mech Eng Part F J Rail Rapid Transit 2009;223:331–43. https://doi.org/10.1243/09544097JRRT234.

[7] Thompson DJ, Jiang J, Toward MGR, Hussein MFM, Dijckmans A, Coulier P, et al. Mitigation of railway-induced vibration by using subgrade stiffening. Soil Dyn Earthq Eng 2015;79:89–103. https://doi.org/10.1016/j.soildyn.2015.09.005.

[8] Grabe PJ. Resilient and permanent deformation of railway foundations under principal stress rotation 2002.

[9] Gräbe PJ, Clayton CR. Effects of Principal Stress Rotation on Permanent Deformation in Rail Track Foundations. J Geotech Geoenvironmental Eng 2009;135:555–65. https://doi.org/10.1061/(ASCE)1090-0241(2009)135:4(555).

[10] Yang LA, Powrie W, Priest JA. Dynamic Stress Analysis of a Ballasted Railway Track Bed during Train Passage. J Geotech Geoenvironmental Eng 2009;135:680–9. https://doi.org/10.1061/(ASCE)GT.1943-5606.0000032.

[11] MADSHUS C, KAYNIA AM. High-speed railway lines on soft ground: Dynamic behaviour at critical train speed. J Sound Vib 2000;231:689–701. https://doi.org/10.1006/jsvi.1999.2647.

[12] Alves Costa P, Calçada R, Silva Cardoso A, Bodare A. Influence of soil non-linearity on the dynamic response of high-speed railway tracks. Soil Dyn Earthq Eng 2010;30:221–35. https://doi.org/10.1016/j.soildyn.2009.11.002.

[13] Shih JY, Thompson DJ, Zervos A. The influence of soil nonlinear properties on the track/ground vibration induced by trains running on soft ground. Transp Geotech 2017;11:1–16. https://doi.org/10.1016/j.trgeo.2017.03.001.

[14] Hegde A, Sitharam TG. Experiment and 3D-numerical studies on soft clay bed reinforced with different types of cellular confinement systems. Transp Geotech 2017;10:73–84. https://doi.org/10.1016/j.trgeo.2017.01.001.

[15] Mezeh R, Mroueh H, Hosseingholian M, Sadek M. New approach for the assessment of train/track/foundation dynamics using in-situ measurements of high-speed train induced vibrations. Soil Dyn Earthq Eng 2019;116:50–9. https://doi.org/10.1016/j.soildyn.2018.10.024.

[16] Fiala P, Degrande G, Augusztinovicz F. Numerical modelling of ground-borne noise and vibration in buildings due to surface rail traffic. J Sound Vib 2007;301:718–38. https://doi.org/10.1016/j.jsv.2006.10.019.

[17] Sayeed MdA, Shahin MA. Three-dimensional numerical modelling of ballasted railway track foundations for high-speed trains with special reference to critical speed. Transp Geotech 2016;6:55–65. https://doi.org/10.1016/j.trgeo.2016.01.003.

[18] Li L, Nimbalkar S, Zhong R. Finite element model of ballasted railway with infinite boundaries considering effects of moving train loads and Rayleigh waves. Soil Dyn Earthq Eng 2018;114:147–53. https://doi.org/10.1016/j.soildyn.2018.06.033.

[19] Mezeh R, Sadek M, Hage Chehade F, Mroueh H. Adaptive meshing scheme for prediction of high-speed moving loads induced ground vibrations. Comput Geotech 2018;100:188–202. https://doi.org/10.1016/j.compgeo.2018.03.014.
[20] Galvín P, Romero A, Domínguez J. Vibrations induced by HST passage on ballast and non-ballast tracks. Soil Dyn Earthq Eng 2010;30:862–73. https://doi.org/10.1016/j.soildyn.2010.02.004.
[21] Kouroussis G, Connolly DP, Forde MC, Verlinden O. Train speed calculation using ground vibrations. Proc Inst Mech Eng Part F J Rail Rapid Transit 2015;229:466–83. https://doi.org/10.1177/0954409713515649.
[22] Lysmer J, Kuhlemeyer RL. Finite dynamic model for infinite media. J Eng Mech Div 1969;95:859–78.
[23] Wu J-J, Whittaker AR, Cartmell MP. The use of finite element techniques for calculating the dynamic response of structures to moving loads. Comput Struct 2000;78:789–99. https://doi.org/10.1016/S0045-7949(00)00055-9.
[24] Wu J-J. Use of equivalent beam models for the dynamic analyses of beamplates under moving forces. Comput Struct 2003;81:2749–66. https://doi.org/10.1016/S0045-7949(03)00341-9.
[25] Koh CG, Chiew GH, Lim CC. A numerical method for moving load on continuum. J Sound Vib 2007;300:126–38. https://doi.org/10.1016/j.jsv.2006.07.038.
[26] Mezeh R, Sadek M, Hage Chehade F, Shahrour I. Adaptive analysis of infinite beams dynamics problems using the periodic configuration update method in the time domain. Int J Numer Anal Methods Geomech 2018;42:618–35. https://doi.org/10.1002/nag.2757.

Figure 1 BPL high-speed line during construction [EIFFAGE rail express]

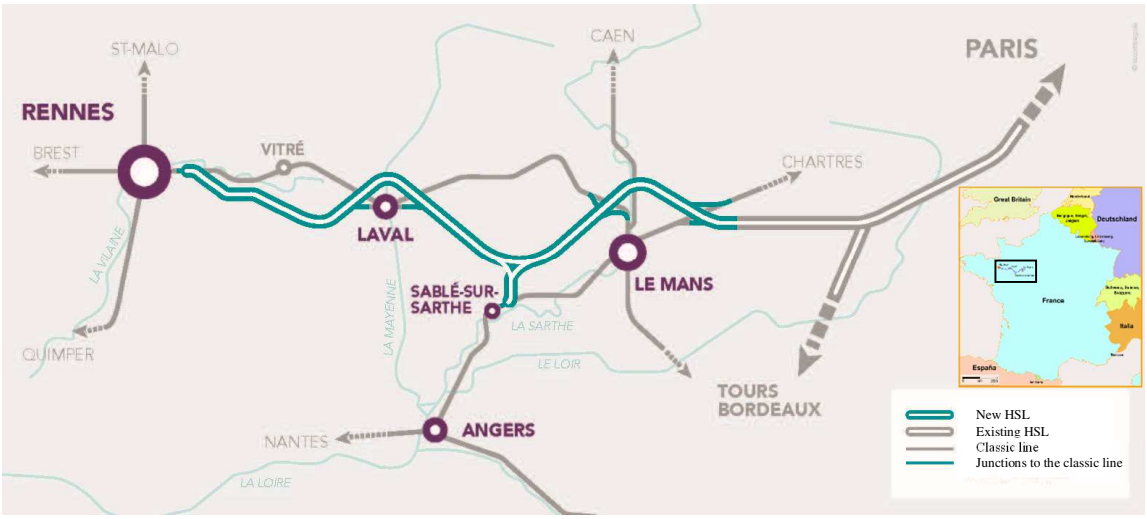

Figure 2 BPL high-speed line within the French network [SNCF Réseau]

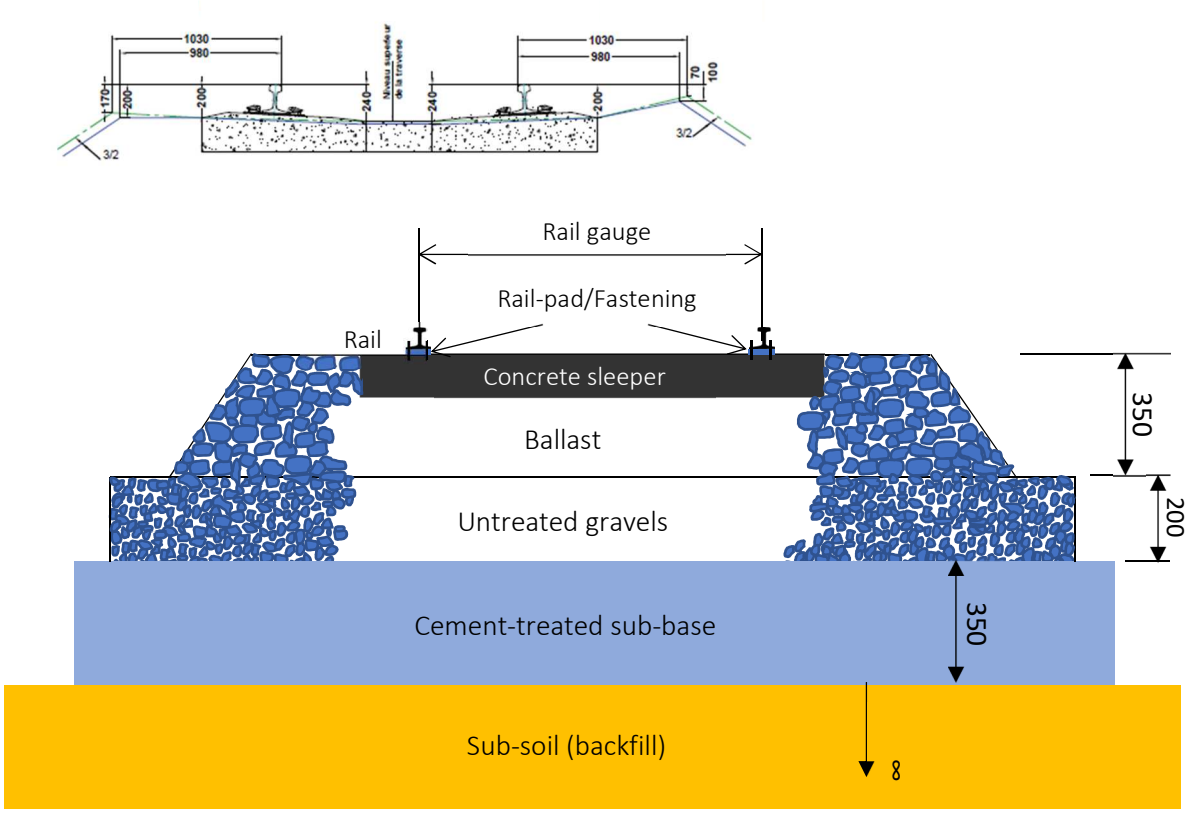

Figure 3 Cross section of the studied ballasted track

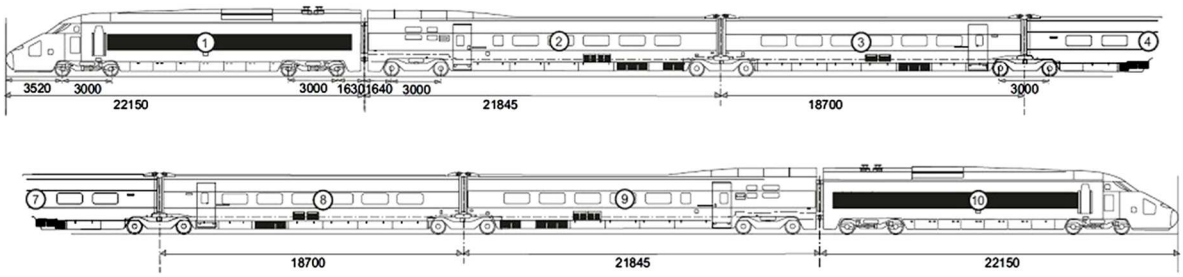

Figure 4 Dimensions of the employed HST during the test period [12]

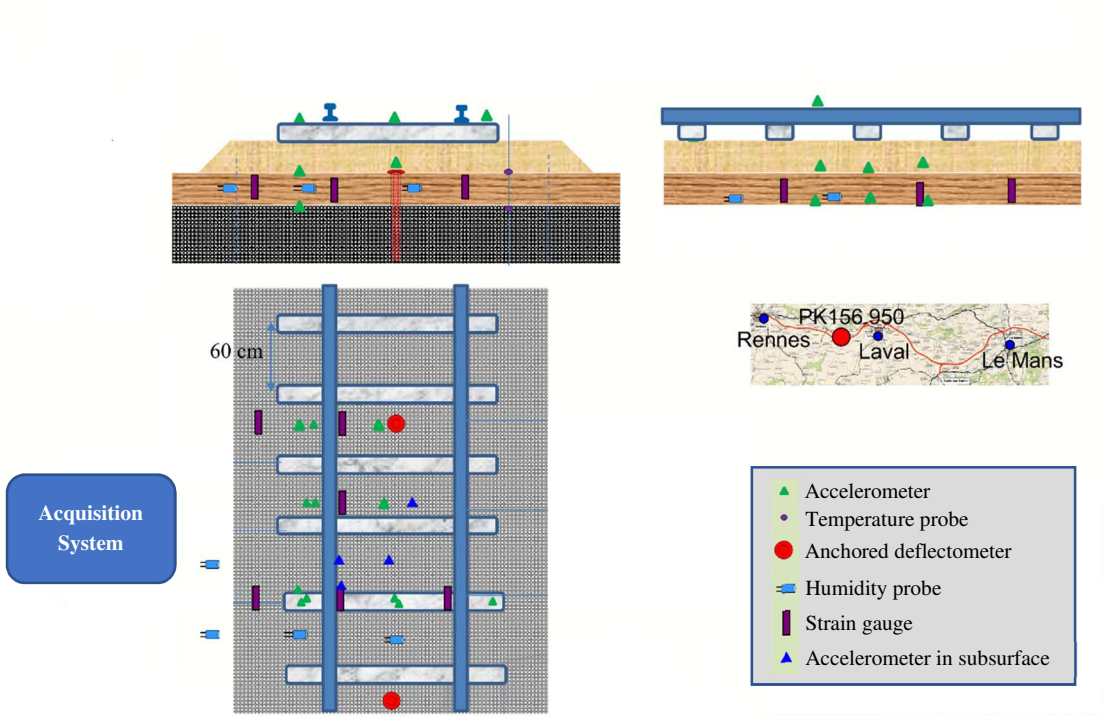

Figure 5 Studied track with the employed sensors

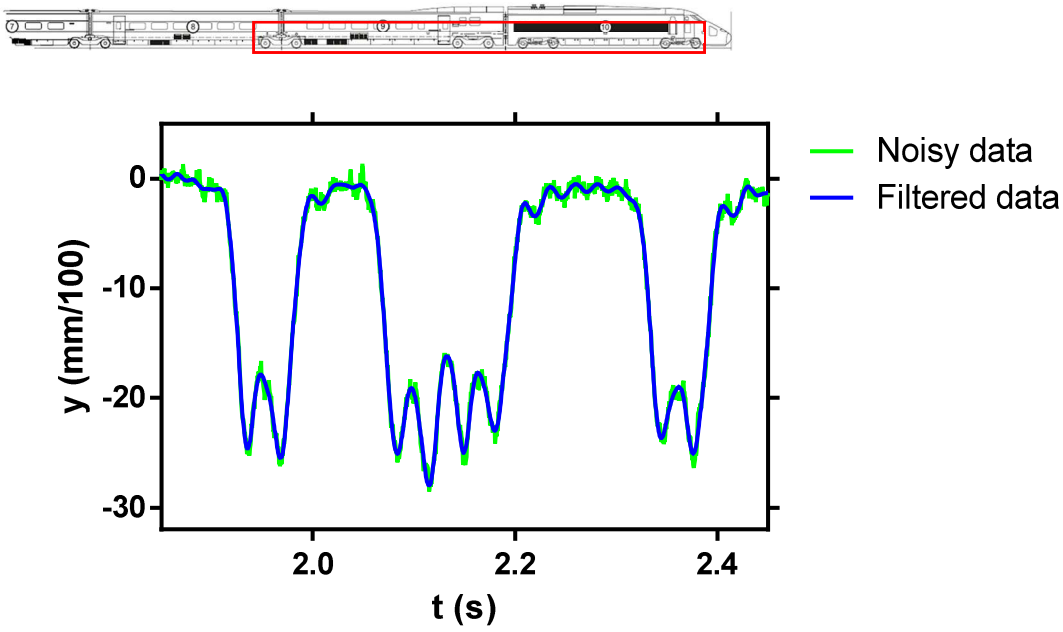

Figure 6 Treated displacement signal using Low-pass filter; cut-off frequency= 63.33 Hz

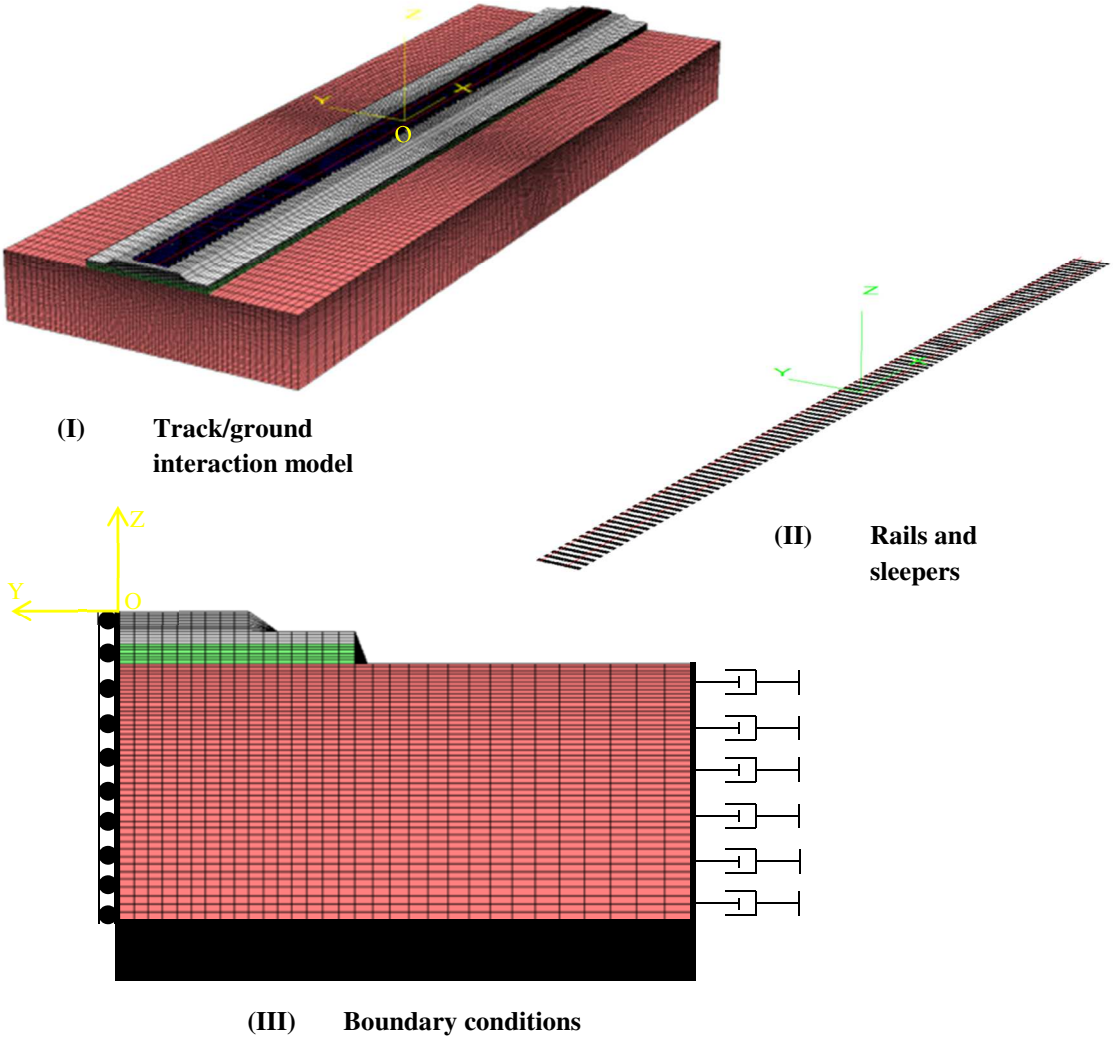

Figure 7 Three-dimensional grid for HST/track/ground dynamics

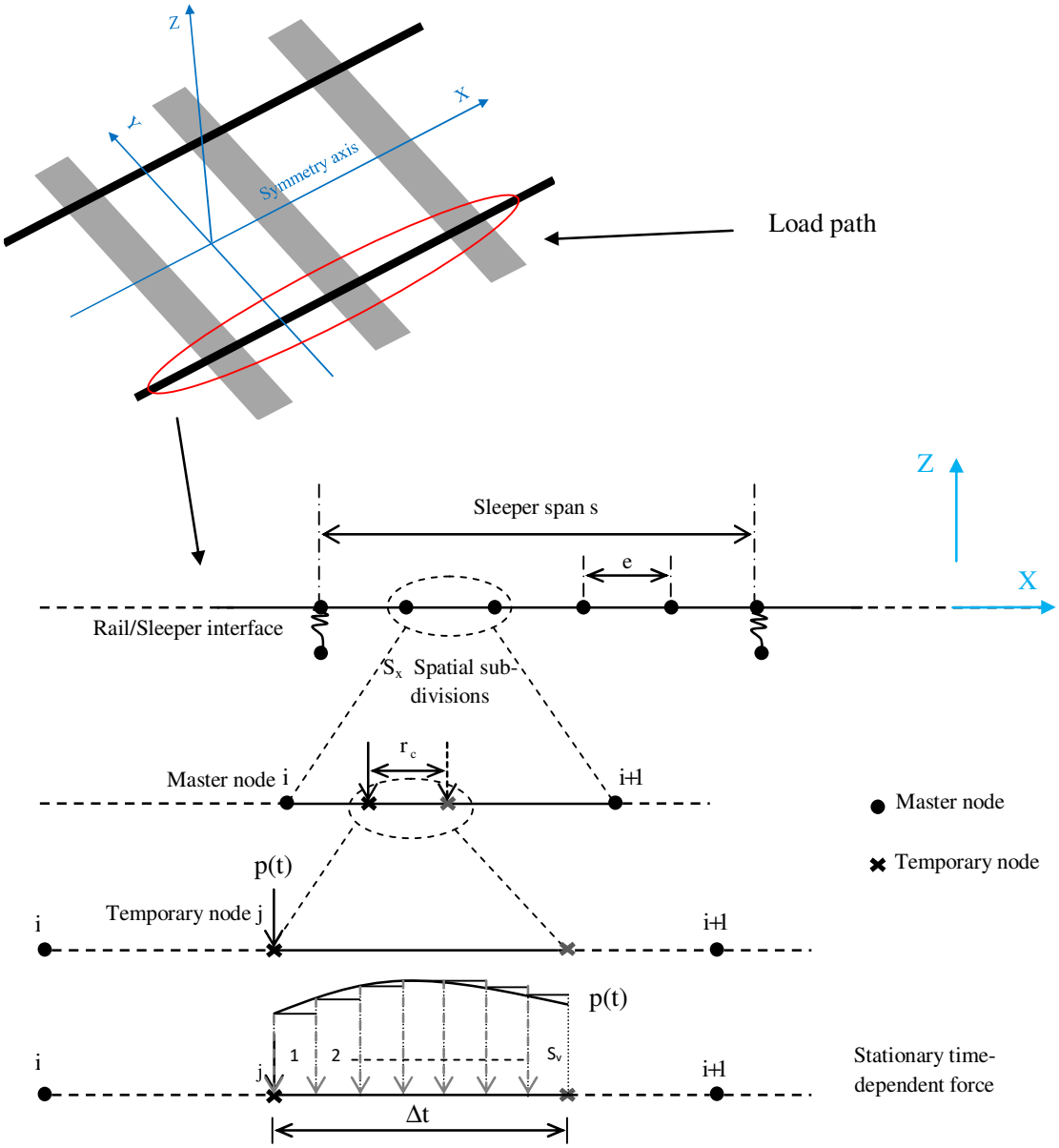

Figure 8 Load-Attached Moving Node (L-AMN) approach for moving load problems [19]

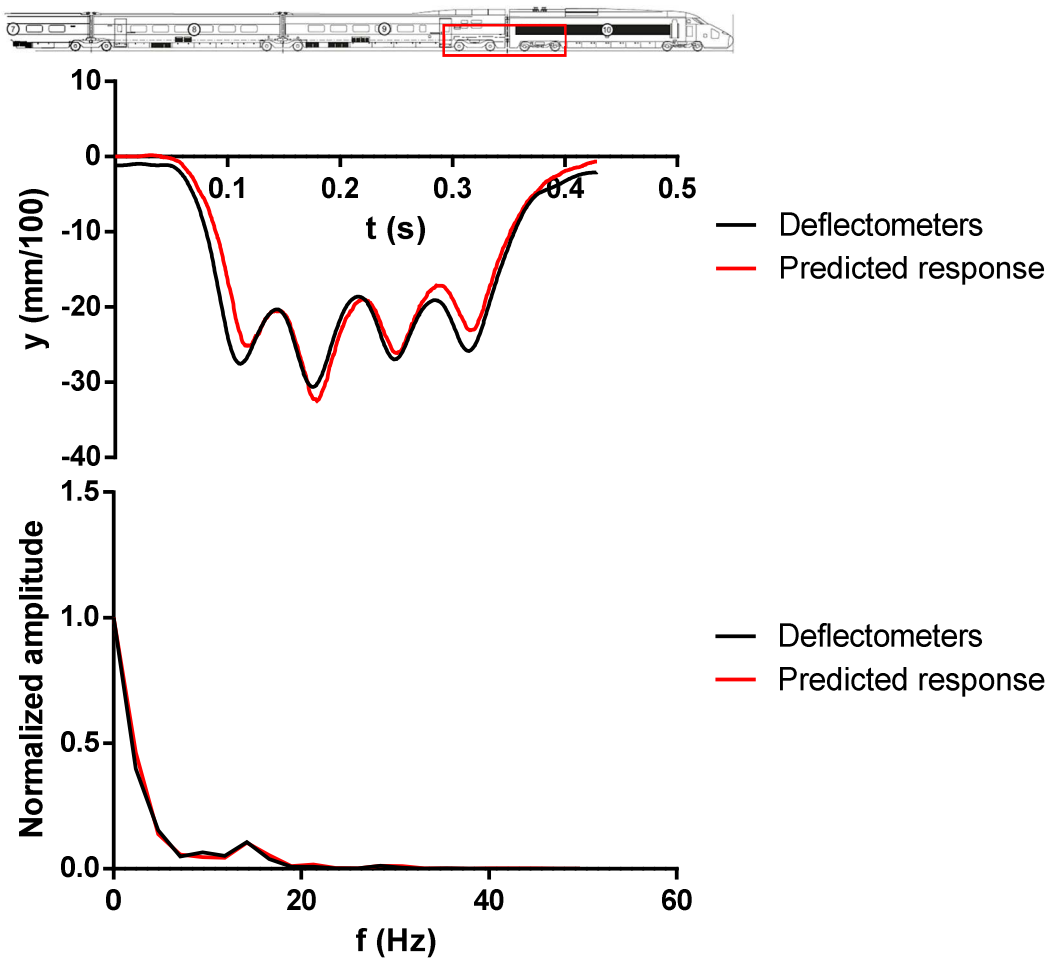

Figure 9 Confrontation between the predicted and the measured responses of the track foundation; case of V= 162 km/h

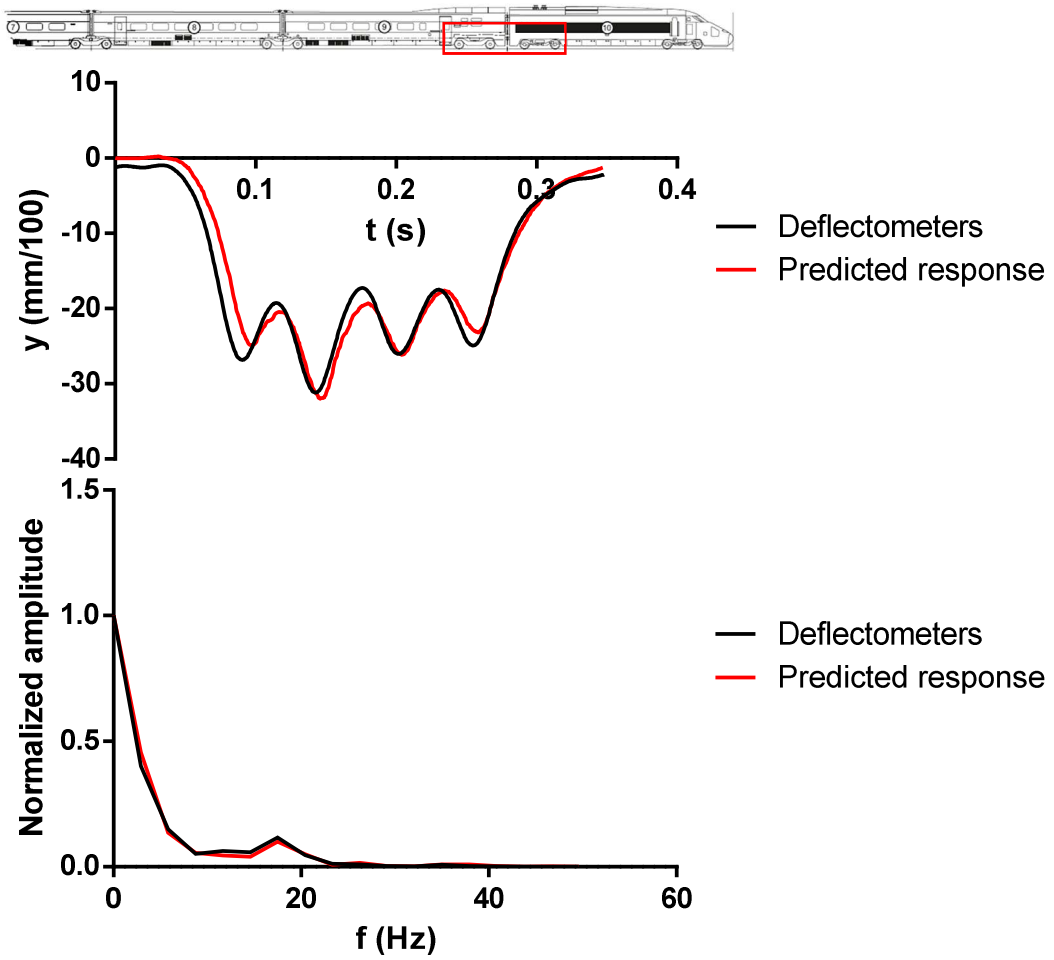

Figure 10 Confrontation between the predicted and the measured responses of the track foundation; case of V= 200 km/h

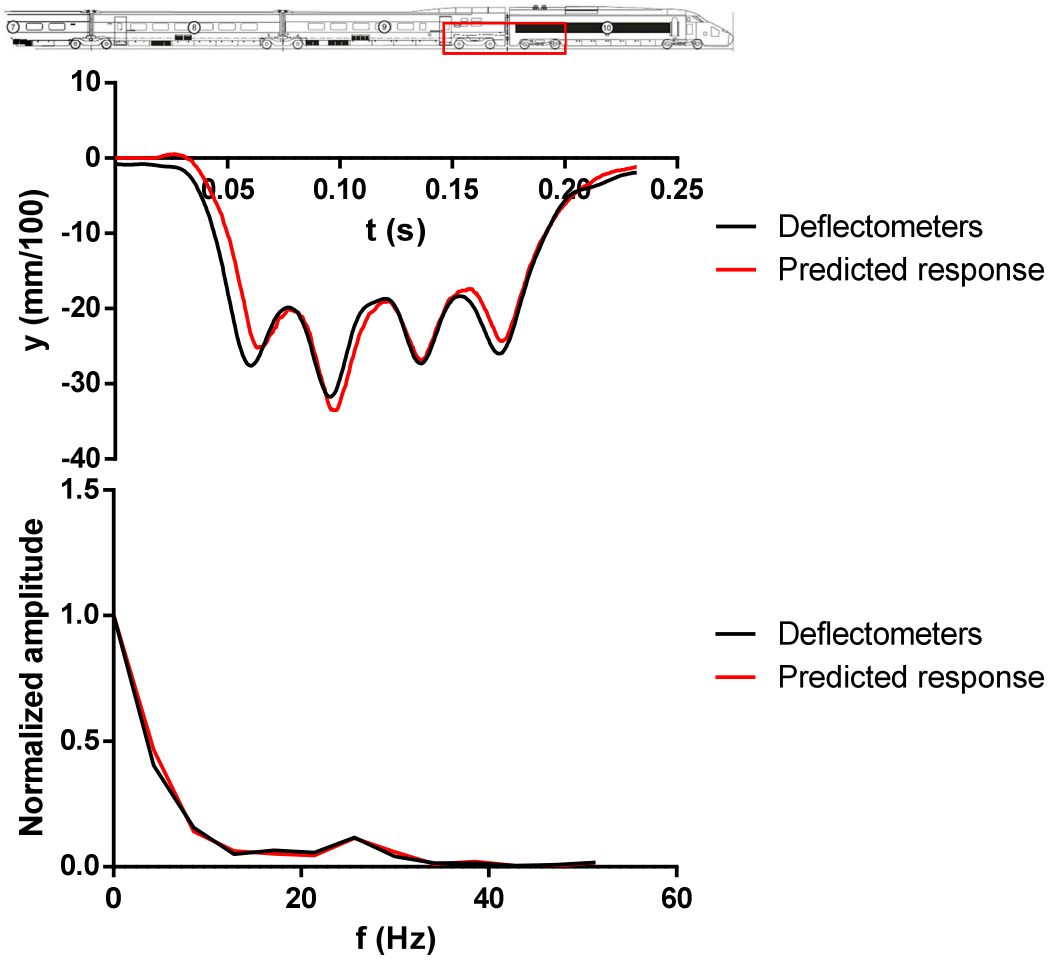

Figure 11 Confrontation between the predicted and the measured responses of the track foundation; case of V= 300 km/h

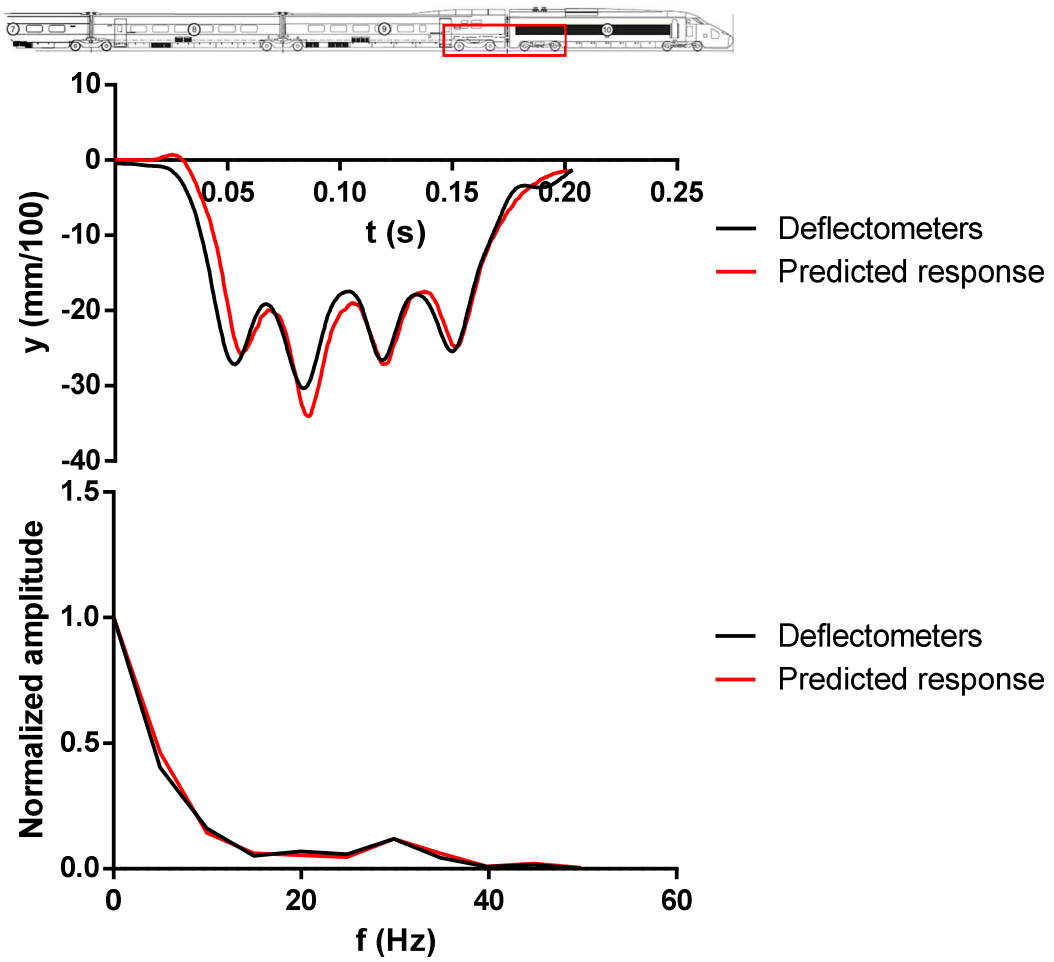

Figure 12 Confrontation between the predicted and the measured responses of the track foundation; case of V= 342 km/h

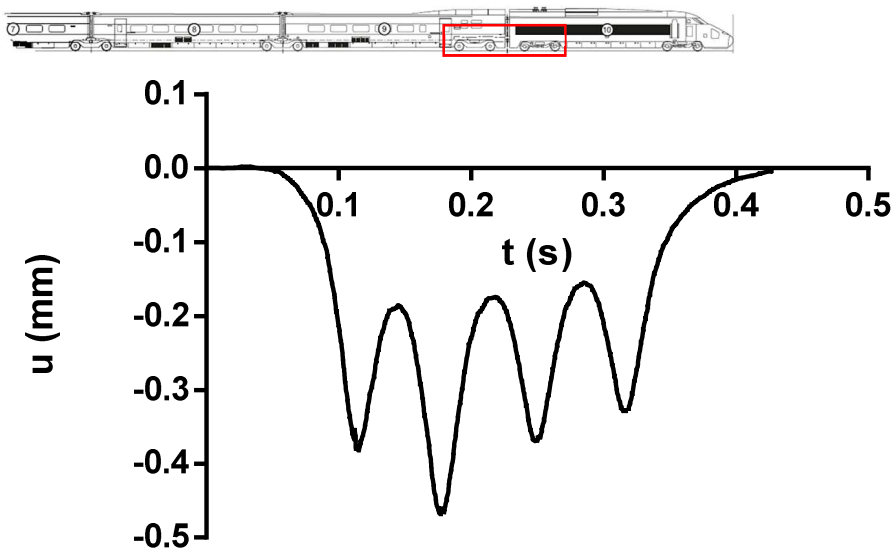

Figure 13 Predicted response of the rail; case of V=162 km/h

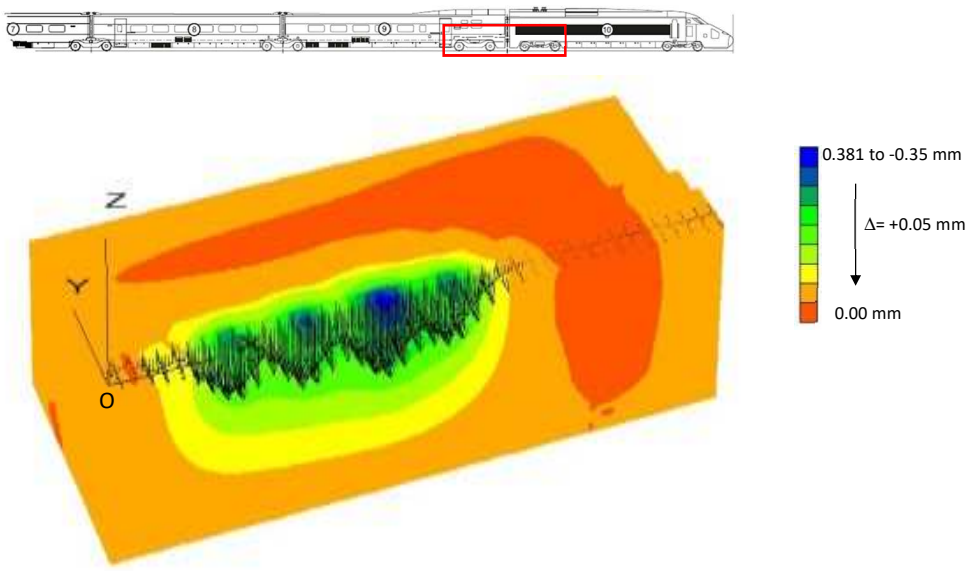

Figure 14 Dynamic response of the interaction model (quarter of the grid) at t= 0.43 s; case of V= 162 km/h